Volume 1 | Number 2 | March 2016 | Pages 83–162

Nanoscale Horizons

The home for rapid reports of exceptional significance in nanoscience and nanotechnology

rsc.li/nanoscale-horizons

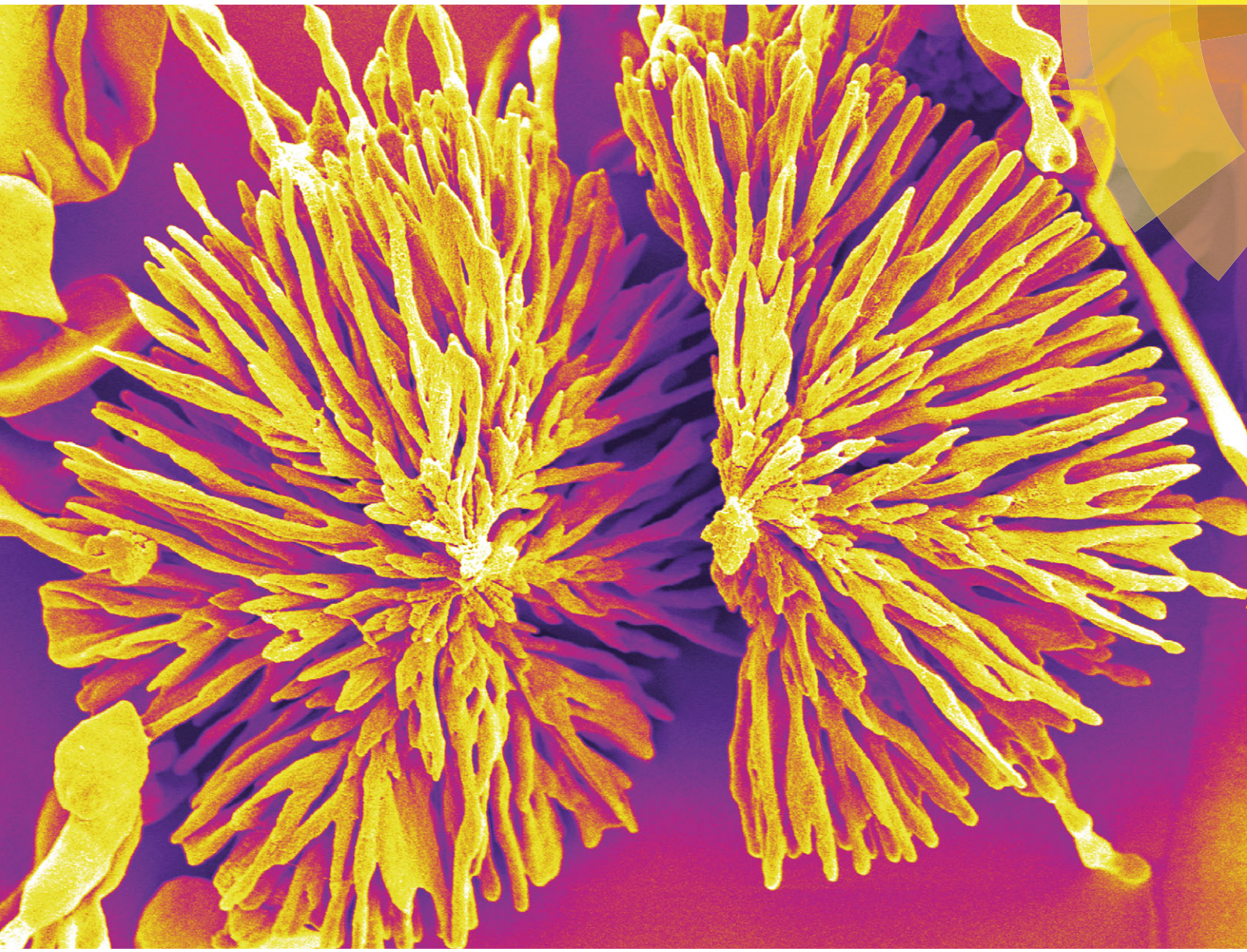

ISSN 2055-6756

ROYAL SOCIETY OF CHEMISTRY

COMMUNICATION

M. Kellermeier, H. Cölfen *et al.*

Functionalisation of silica–carbonate biomorphs

NCNST

Nanoscale Horizons

COMMUNICATION

View Article Online
View Journal | View Issue

Functionalisation of silica–carbonate biomorphs†

J. Opel,[a] F. P. Wimmer,[a] M. Kellermeier*[b] and H. Cölfen*[a]

Cite this: *Nanoscale Horiz.*, 2016, **1**, 144

Received 22nd October 2015,
Accepted 11th January 2016

DOI: 10.1039/c5nh00094g

rsc.li/nanoscale-horizons

Biomorphs are a unique class of self-organised silica–carbonate mineral structures with elaborate shapes. Here we report first approaches to modify these complex inorganic architectures through silane chemistry, binding of nanoparticles, and organic polymerisation. This leads to functional nanostructures in which the complexity of the originally inorganic template is preserved, and offers new diagnostic tools to study the mechanisms underlying their formation.

Conceptual insights

Biomorphs are a unique class of self-organised nanostructured silica–carbonate mineral structures with elaborate shapes. This complexity of shapes is otherwise only formed in the living world in form of biominerals. We want to utilize the unique inorganic biomorph structures to add function to create nanostructured materials with complex shape and new and emergent properties. Here we report first approaches to modify these inorganic architectures through silane chemistry, binding of nanoparticles, and organic polymerisation. This leads to functional nanostructures in which the complexity of the originally inorganic template is preserved. The reported three examples already show the large variability of our approach and especially the post functionalization with silanes provides the possibility to attach a variety of functional nanoparticles. Therefore, our study introduces a new and variable platform towards novel functional nanostructured materials with complex shapes.

Crystallisation of alkaline-earth metal carbonates in the presence of silica at high pH can result in fascinating hybrid structures with curved morphologies and ordered textures across several length scales.[1] These so-called "biomorphs" consist of innumerous carbonate nanocrystals that are stabilised by co-precipitating silicate species and self-assemble into delicate forms like regular helicoids or sinuous sheets, which may eventually become sheathed by an outer skin of silica on the micron level.[2] Despite the absence of any organic matter, the obtained structures closely mimic biomineral frameworks produced by living organisms[3] and moreover resemble some of the oldest putative microfossils.[4] Therefore, biomorphs have been used as a model system to study biomimetic self-organisation[5] and serve as a vital proof that complex curved forms are not exclusive to the living world.[6]

Over the past ten years, the mechanism for the formation of these unusual inorganic–inorganic hybrid structures has been investigated in depth, leading to a meanwhile convergent picture of autocatalytic reaction coupling being the driving force for self-assembly at the nanoscale.[7,8] In particular, it was shown that local changes in pH at the growth front trigger the dynamic co-mineralisation of silica and carbonate due to their inverse trends of solubility with pH, as depicted schematically in Fig. 1a–c and described in more detail elsewhere.[9] The result is an array of crystalline carbonate nanoparticles (dark-grey rods in Fig. 1) embedded in a more or less continuous matrix of amorphous silica (light-grey domains in Fig. 1c), which subsequently evolves free from crystallographic constraints towards curved superstructures.[10]

Even though biomorphs exhibit many interesting features in terms of structure and morphology, they still consist of plain inorganic compounds (usually $BaCO_3$ and SiO_2) and thus bear little to no distinct functionality. To address this issue and widen the scope of biomorphs towards materials science, we have started to chemically modify the inorganic nanostructures, either *in situ* during their formation or by post-treatment. Here we present three different approaches to achieve "functional" biomorphs: (1) silane co-condensation, (2) immobilisation of metal nanoparticles and quantum dots, and (3) organic polymerisation. All three concepts yield hybrid materials with enhanced functionality and equal structural complexity as inherited from the self-assembly process of biomorphs.

[a] *Physical Chemistry, University of Konstanz, Universitätsstrasse 10, D-78464 Konstanz, Germany. E-mail: helmut.coelfen@uni-konstanz.de; Fax: +49 7531 88 3139; Tel: +49 7531 88 4063*
[b] *Material Physics, BASF SE, GMC/O – B007, Carl-Bosch-Strasse 38, D-67056 Ludwigshafen, Germany. E-mail: matthias.kellermeier@basf.com; Fax: +49 621 66 43388; Tel: +49 621 60 43388*

† Electronic supplementary information (ESI) available: Details on experimental procedures (Sections S1 and S2), quantification of the degree of thiol functionalisation (Section S3, with Fig. S1), estimation of the gold nanoparticle loading on biomorphs (Section S4, with Fig. S2), Raman and IR analyses of polymer-functionalised biomorphs (Section S5, with Fig. S3). See DOI: 10.1039/c5nh00094g

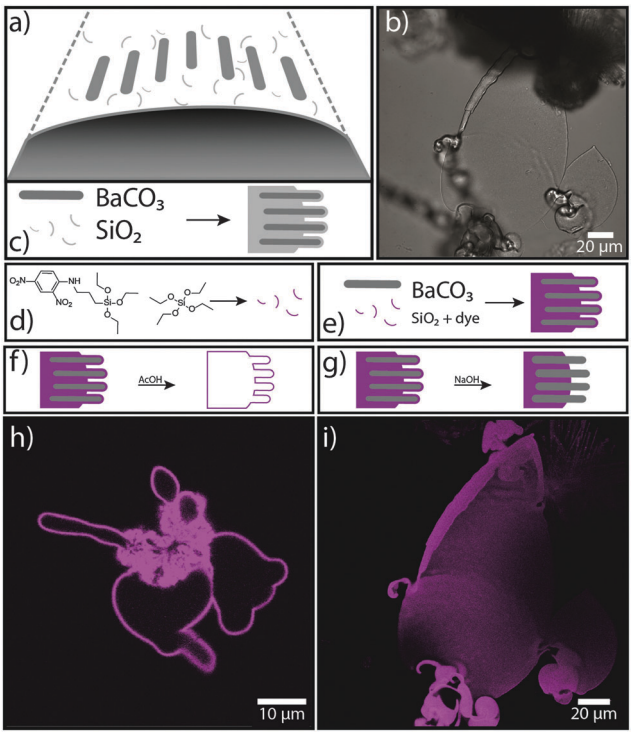

Fig. 1 *In situ* functionalisation of biomorphs by silane co-condensation. (a) Schematic drawing of the growth of a biomorph by the continuous formation of carbonate nanocrystals (dark-grey rods) in the presence of silicate species (thin light-grey threads). (b) CLSM image (transmission channel) of a biomorph sheet. (c) Co-precipitation of $BaCO_3$ nanocrystals and unfunctionalised amorphous silica. (d) Co-condensation of TEOS and DNPTES into fluorescent "functional" silica. (e) Incorporation of fluorescently labeled silanes into the siliceous component of biomorphs (magenta-coloured domains). (f) Selective dissolution of the carbonate component by acid post-treatment, leading to a hollow silica structure. (g) Partial dissolution of the (outer) silica component by NaOH post-treatment. (h and i) CLSM images (fluorescence channel) of functional biomorphs after acid and base treatment, respectively.

The idea behind approach (1) was to selectively modify the silica component in biomorphs and introduce functional groups *via* alkoxysilane chemistry.[11] In fact, Voinescu *et al.* have shown that biomorphs can be formed with tetraethoxysilane (TEOS) as an alternative organic silica source instead of commonly used inorganic water glass (sodium silicate solution).[12] To obtain typical biomorphic structures, the TEOS (*ca.* 9 mM) was pre-hydrolysed in water with sodium hydroxide before adding Ba^{2+} ions (5 mM) to the alkaline solution (pH 10–11) and inducing crystallisation by exposure to atmospheric CO_2. Based on this recipe, we grew biomorphs from mixtures of TEOS and functional triethoxysilanes like 3-mercaptopropyltriethoxysilane (3-MPTES, for introducing thiol groups), 3-aminopropyltriethoxysilane (3-APTES, for amine groups) and 3-(2,4-dinitrophenylamino)propyltriethoxysilane (DNPTES, carrying a fluorescent label) (see Sections S1 and S2 in the ESI† for experimental details). Fig. 1 summarises the results of an experiment in which 5 vol% of TEOS were replaced by DNPTES. Confocal laser scanning microscopy (CLSM) images (Fig. 1h and i) clearly evidence that the obtained biomorphs display strong fluorescence, demonstrating successful incorporation of the functional silane into the structure in a one-pot synthesis.

Bright and homogeneous fluorescence signal from all parts of the aggregates moreover suggests that co-condensation of TEOS and DNPTES leads to a statistical distribution of the fluorescent dye in the silica component of the biomorph, showing that this simple method enables a complete functionalisation of the entire structure. Apart from that, the incorporation of fluorescent groups allows the siliceous component to be easily detected and located. As already mentioned above, silica can be present both as an external skin and – to a greater or lesser extent – also in the bulk material around and in-between the carbonate nanocrystals. This can be analysed in detail by selective dissolution experiments.[6] For example, by immersing the as-grown aggregates into dilute acid (0.03 M HOAc), the carbonate component can be removed quantitatively within minutes. This leaves a hollow structure of fluorescent silica (Fig. 1f and h), corresponding to the thick outer skin covering the whole crystal assembly. On the other hand, treatment with base (1 M NaOH) dissolves this outer skin and exposes the inner carbonate-rich core (Fig. 1g and i). Owing to the fluorescent label, we are now able to confirm that silica is also an integral part of the inner structure (which is still under debate[2]), where it presumably serves as a "glue" holding the carbonate crystals together. The fact that this part of the silica was not dissolved in NaOH indicates that it is intimately associated to the carbonate phase – which is well in line with the proposed model of autocatalytic co-mineralisation of the two components at the nanoscale.[7,8] We note that pre-hydrolysis of the silanes proved to be crucial to obtain characteristic biomorphic structures directly in solution. This emphasises the key role of silica speciation in the process of morphogenesis.

Besides the above-described *in situ* functionalisation of biomorphs by co-condensation of alkoxysilanes with TEOS, we also conducted post-functionalisation experiments with already grown structures. Freshly harvested biomorphs are expected to carry free silanol groups at the surface of their outer silica skin (Fig. 2a and b), to which functional silanes can be coupled *via* well-known surface modification methods.[13] In this way, a broad range of functional groups can be imparted on the biomorphs, as illustrated by Fig. 2.

Using the fluorescent silane DNPTES (Fig. 2c), structures similar to those in Fig. 1 were obtained, but in this case, no fluorescence could be detected in the inner part (after treatment with 1 M NaOH), indicating that only the silica in the outer skin is accessible for silane coupling. Nevertheless, bright fluorescence from the outer parts confirms that surface functionalisation by post-treatment is possible. Based on these results, further functional groups were tested. For instance, amine groups were introduced by the silane 3-APTES (Fig. 2d); their presence at the surface was confirmed by direct coupling of isothiocyanate dyes like FITC (fluorescein isothiocyanate),[14] which were subsequently again detected *via* their fluorescence (*cf.* CLSM image in Fig. 2d). Other organic compounds can be coupled to the amine groups on the biomorph surface in the same way. Post-functionalisation of the structures with thiol groups was performed using the silane 3-MPTES (Fig. 2e). The presence of surface-bound thiol

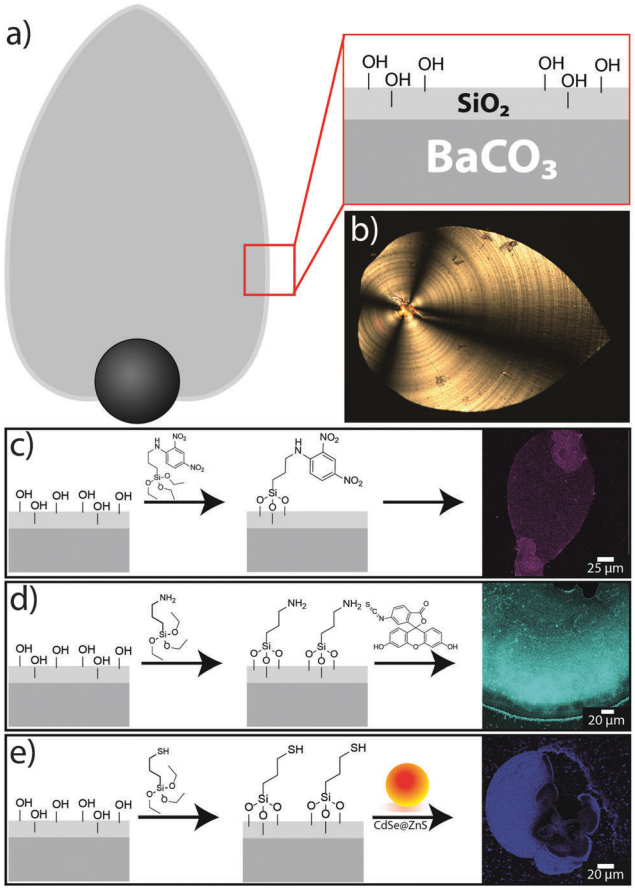

Fig. 2 Post-functionalisation of biomorphs with different trialkoxysilanes. (a) Schematic drawing of a biomorph sheet with a thick outer silica skin carrying free silanol groups accessible for coupling reactions. (b) Polarised optical micrograph of a typical biomorph sheet. (c–e) Schemes for the post-silanisation of as-grown biomorphs with (c) DNPTES, (d) 3-APTES and further functionalisation with FITC, (e) 3-MPTES and subsequent binding of CdSe@ZnS quantum dots. In all cases, successful functionalisation is proven by corresponding CLSM images (right).

groups was verified with Ellman's reagent,[15] which forms nitrothiobenzoate (NTB) adducts in slightly alkaline solutions that can be detected and quantified by their absorption at 408 nm. With the recipe used in this study, about 1 µmol g^{-1} thiol groups could be anchored on the biomorphs (see Section S3 and Fig. S1 in the ESI† for details).

Having shown that biomorphs can readily be functionalised by either *in situ* or post-silanisation, we now turn to approach (2) of our work, *i.e.* the immobilisation of functional nanoparticles on the surface of the aggregates. To achieve this, we made use of the thiol-bearing biomorphs obtained as described above (Fig. 2e), since SH groups have a strong affinity to bind to certain metals and minerals. As a proof of concept, two distinct types of nanoparticles were chosen here: CdSe@ZnS core–shell quantum dots (QDs), about 9 nm in diameter (with d_{core} = 4 nm), and spherical gold nanoparticles (AuNPs) with an average size of 14 nm. In both cases, the thiol-modified biomorphs were incubated in dispersions of the nanoparticles for several hours and rinsed afterwards to remove any loosely adhering material. Fig. 2e shows the result for a biomorph that was exposed to the quantum dots. The strong fluorescence from the flat part of the sheet-like structure demonstrates successful immobilisation of the QDs at the surface (note that the black regions within the structure in the CLSM image are not in the confocal plane and hence do not show fluorescence here). In addition, the presence of cadmium and zinc was verified by EDX measurements (atomic ratio: Ba : Si : Zn : Cd = 1 : 0.6 : 0.05 : 0.01). In the case of the AuNPs, surface modification cannot be directly confirmed by fluorescence microscopy. While EDX analyses traced certain amounts of gold at the surface (atomic ratio: Ba : Si : Au = 0.94 : 1 : 0.01), two further methods were used to study the prepared hybrid materials. First, the biomorphs were crushed after functionalisation and investigated by means of transmission electron microscopy (TEM). The resulting images show small AuNPs covering the larger silica spheres (see Fig. S2a in the ESI†), supporting the assumption that the metal nanoparticles bind to the thiol groups at the silica surface. Second, we used catalytic reactions to prove the presence of AuNPs on the structures without destroying them (Fig. 3). The chosen test reactions were the reduction of 4-nitrophenol (pNP) with sodium borohydride[16] and the reduction of resazurin with hydroxylamine (*cf.* Fig. 3c).[17,18] In the latter case, the formed resorufin could easily be observed by CLSM as a strongly fluorescent area around the biomorphic structures (Fig. 3b), suggesting that the reaction occurred directly on the surface where the AuNPs were immobilised (note that unfunctionalised structures did not show this behaviour). The resazurin-to-resorufin reaction also occurred without AuNP-

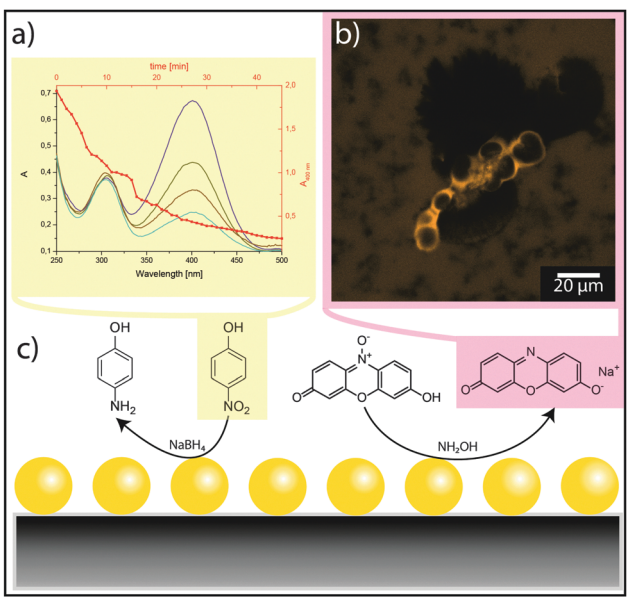

Fig. 3 Catalytic reactions with AuNPs immobilised on biomorphs. (a) UV-Vis spectra showing the reduction of *p*-nitrophenol by $NaBH_4$. (b) CLSM image of a AuNP-bearing biomorph in a solution of resazurin and hydroxylamine. The formation of the reduced state (resorufin) can be detected by enhanced fluorescence at the surface of the biomorph. (c) Schematic drawing of the two test reactions using the immobilised particles as catalyst. The coloured molecules were analytically observed.

bearing biomorphs, but at a much slower rate. This shows that the surface-bound gold particles act as a catalyst in this reaction, hence imparting distinct functionality to the biomorph structure.

The reduction of pNP by $NaBH_4$ in the presence of gold-functionalised biomorphs was traced by UV/Vis spectroscopy (Fig. 3a). In particular, the strong absorption band of pNP at 400 nm was used to monitor the progress of the reaction. The thick red line in Fig. 3a shows the change in the peak area as a function of time. It is evident that functional biomorph structures can efficiently catalyse this reaction as well (note that pNP is not reduced by $NaBH_4$ in the absence of Au). Based on reaction rates derived from similar tests under various conditions, and by using the EDX results for intact AuNP@Biomorph structures as well as UV-Vis data from gold colloid dispersions, the loading of Au nanoparticles on the inorganic template was determined to be in a range of 0.03–0.7 nmol g^{-1} (see Section S4 and Fig. S2 in ESI†). Taken together, the experiments described above clearly illustrate that functional nanoparticles can be immobilised on biomorphs, and that this yields complex ternary hybrid nanostructures with interesting catalytic properties.

Finally, in approach (3), we made attempts to coat and/or fill as-grown biomorphs by a polymer, so as to imprint the structure of the hard inorganic template into soft organic material (Fig. 4). In order to avoid uncontrolled bulk polymerisation, it is necessary to have a monomer that first binds onto the silica–carbonate aggregates and then polymerises in and/or around the inorganic architecture. A suitable candidate in this context is 10,12-pentacosadiynoic acid (PCDA), a monomer showing strong affinity to bind on carbonate surfaces *via* its carboxyl groups.[19] Moreover, PCDA polymerisation can be conveniently triggered by exposure to UV light (*cf.* Fig. 4e).

Thus, we removed the outer silica skin from native biomorphs by leaching in 1 M NaOH and subsequently incubated the exposed carbonate core in a solution of PCDA. After replacing the supernatant, the PCDA adsorbed on the biomorphs was polymerised by illumination at 365 nm. SEM images of the resulting structures (Fig. 4c) show that the treated biomorphs (a worm-like morphology in the present example) had a rougher appearance than their native analogues (Fig. 4a) and were more or less completely covered by a material with flake-like morphologies typical for poly(PCDA). This notion is corroborated by optical micrographs of the samples (Fig. 4d), in which the biomorphs display a blue-coloured rim, again characteristic of polymerised PCDA (note that poly(PCDA) can exist in two distinct forms, one blue and one red, between which the polymer can switch upon heating or cooling).[20,21]

The presence of poly(PCDA) on the crystal aggregates could furthermore be clearly demonstrated by IR and Raman analyses of biomorphs before and after functionalisation (see Section S5 and Fig. S3 in the ESI†). Another beneficial property of PCDA is that its polymerised form shows significant fluorescence. This allowed us to localise the polymer in the as-obtained hybrids by confocal microscopy. Corresponding images (Fig. 4b) reveal that the polymerisation process led to the formation of a continuous organic shell around the biomorphs (as confirmed by *Z*-stacking image series) – or in other words, that the morphology of the inorganic architecture was transferred to the emerging organic phase. Actually, this situation is inverse to common biological and biomimetic mineralisation, where usually an organic template controls the shape (and structure) of a forming inorganic phase.[22] On the other hand, our analyses suggest that polymerisation did not occur in the bulk volume of the biomorphs (*cf.* Fig. 4b), presumably due to insufficient infiltration of the PCDA monomer into the dense nanostructure. This becomes further evident when the carbonate core is dissolved in acid, leaving hollow polymer shells behind.

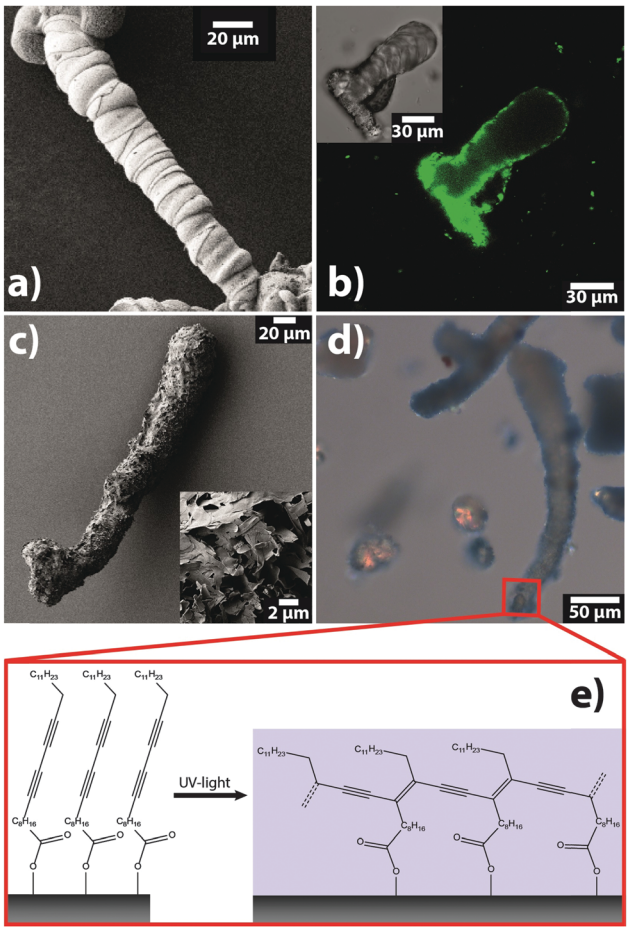

Fig. 4 Organic polymerisation on biomorphs. (a) SEM image of a structure with worm-like morphology before functionalisation. (b) CLSM images (main window: fluorescence channel ($\lambda_{exc.}$ = 561 nm), inset: transmission channel) of another worm-like structure after functionalisation. (c) SEM image of a poly(PCDA)-coated worm. The inset shows a zoom on the surface of the aggregate, revealing the flake-like character of the polymer coating. (d) Optical micrograph of biomorphs after functionalisation, showing the characteristic blue colour of poly(PCDA). (e) Schematic drawing of the polymerisation of PCDA molecules adsorbed on the biomorph surface.

Conclusion

In summary, our results highlight different approaches to add functionality to self-organised silica–carbonate structures

by rather straightforward means. We have shown that silane chemistry serves as a versatile toolbox for molecular functionalisation of the silica component in biomorphs, either by direct co-condensation during self-assembly or afterwards through surface modification, while in both cases the complex ultrastructures of the inorganic–inorganic hybrids are preserved. This represents a notable and non-trivial achievement when considering that even slightest variations in the growth conditions can change the shape and texture of biomorphs dramatically.[12] These experiments have provided new insights into the role and distribution of silica in the aggregates by direct visualisation *via* fluorescent labeling. Apart from such structural information, biomorphs carrying dinitrophenyl groups could be interesting materials for the field of non-linear optics (NLO):[23,24] DNPTES-labeled silica is known to exhibit second order non-linearity due to the non-centrosymmetric environment, and hence it should show second harmonic generation (SHG) phenomena if the dyes are aligned.[24,25] In addition to fluorescent labeling, post-silanisation of biomorphs also allows for anchoring various functional groups such as amines or thiols at the surface, which can then be used for further functionalisation. In the present work, this strategy was employed to generate biomorph-based superstructures of semiconductor and metal nanoparticles as first examples to demonstrate the variability of our approach. The resulting materials may show special optical properties, for instance through the coupling of the surface plasmons of nanoparticles immobilised on helicoidal structures,[1,2,4–10] leading to chiral plasmonics on single biomorphs.[26,27] We are furthermore confident that also other functional materials can be bound to the biomorph surfaces in a similar way. In particular, it would be desirable to orient magnetic or electric dipoles along the sinuous landscape provided by the inorganic template, as this is expected to produce complex couplings and thus give rise to new physical properties. For example, oriented attachment of suitable magnetic nanoparticles (such as iron oxides) on existing biomorph architectures could lead to long-range ordered superstructures through self-assembly,[28,29] which in the case of twisted morphologies may yield micropropellers capable of navigating in an applied external magnetic field.[30,31] In turn, electric dipole coupling could be realised by using anisotropic semiconductor nanoparticles like zinc oxide.[32] Finally, selective dissolution of the inner carbonate core gives easy access to hollow frameworks of functional materials with complex shapes and additional possible advantages in terms of properties and applications.[33]

Post-functionalisation thus appears to be a simple and universal method with great potential to benefit from the unique structures of biomorphs in the design of nanoparticle assemblies with new collective and emergent properties, which remain to be explored. Along the same lines, it is possible to shape organic matter by *in situ* polymerisation of suitable pre-adsorbed monomers on the inorganic architectures. This bears fascinating – though inverted – analogies to biomineralisation and may have profound implications for primitive life detection[4,6] as well as the early evolution of increasingly complex organic matter.

Acknowledgements

The authors thank Profs. Clément Sanchez and Werner Kunz for valuable discussions and suggestions for this work. In addition, we are grateful to Tjaard de Roo for providing the quantum dots, Tuan Anh Pham and Holger Reiner for the gold colloids, Shengtong Sun for help with the PCDA experiments, Mathias Altenburg for performing Raman microscopy, and the Bioimaging Center of the University of Konstanz for access to their instruments.

References

1 M. Kellermeier, H. Colfen and J. M. Garcia-Ruiz, *Eur. J. Inorg. Chem.*, 2012, 5123–5144.
2 M. Kellermeier, E. Melero-Garcia, F. Glaab, J. Eiblmeier, L. Kienle, R. Rachel, W. Kunz and J. M. Garcia-Ruiz, *Chem. – Eur. J.*, 2012, **18**, 2272–2282.
3 S. Weiner and L. Addadi, *Annu. Rev. Mater. Res.*, 2011, **41**, 21–40.
4 J. M. Garcia-Ruiz, S. T. Hyde, A. M. Carnerup, A. G. Christy, M. J. Van Kranendonk and N. J. Welham, *Science*, 2003, **302**, 1194–1197.
5 W. L. Noorduin, A. Grinthal, L. Mahadevan and J. Aizenberg, *Science*, 2013, **340**, 832–837.
6 J. M. Garcia Ruiz, A. Carnerup, A. G. Christy, N. J. Welham and S. T. Hyde, *Astrobiology*, 2002, **2**, 353–369.
7 J. M. García-Ruiz, E. Melero-García and S. T. Hyde, *Science*, 2009, **323**, 362–365.
8 M. Kellermeier, E. Melero-García, W. Kunz and J. M. García-Ruiz, *J. Colloid Interface Sci.*, 2012, **380**, 1–7.
9 J. Opel, M. Hecht, K. Rurack, J. Eiblmeier, W. Kunz, H. Colfen and M. Kellermeier, *Nanoscale*, 2015, **7**, 17434–17440.
10 M. Kellermeier, J. Eiblmeier, E. Melero-García, M. Pretzl, A. Fery and W. Kunz, *Cryst. Growth Des.*, 2012, **12**, 3647–3655.
11 L. Nicole, L. Rozes and C. Sanchez, *Adv. Mater.*, 2010, **22**, 3208–3214.
12 A. E. Voinescu, M. Kellermeier, A. M. Carnerup, A.-K. Larsson, D. Touraud, S. T. Hyde and W. Kunz, *J. Cryst. Growth*, 2007, **306**, 152–158.
13 C. G. Golander and E. Kiss, *Colloids Surf., A*, 1993, **74**, 217–222.
14 J. L. Riggs, R. J. Seiwald, J. H. Burckhalter, C. M. Downs and T. G. Metcalf, *Am. J. Pathol.*, 1958, **34**, 1081–1097.
15 G. L. Ellman, *Arch. Biochem. Biophys.*, 1959, **82**, 70–77.
16 J. Lee, J. C. Park and H. Song, *Adv. Mater.*, 2008, **20**, 1523–1528.
17 W. Xu, J. S. Kong, Y.-T. E. Yeh and P. Chen, *Nat. Mater.*, 2008, **7**, 992–996.
18 G. De Cremer, B. F. Sels, D. E. De Vos, J. Hofkens and M. B. Roeffaers, *Chem. Soc. Rev.*, 2010, **39**, 4703–4717.
19 A. Berman, D. J. Ahn, A. Lio, M. Salmeron, A. Reichert and D. Charych, *Science*, 1995, **269**, 515–518.
20 S. Dei, A. Matsumoto and A. Matsumoto, *Macromolecules*, 2008, **41**, 2467–2473.
21 J. B. Pang, L. Yang, B. F. McCaughey, H. S. Peng, H. S. Ashbaugh, C. J. Brinker and Y. F. Lu, *J. Phys. Chem. B*, 2006, **110**, 7221–7225.

22 F. C. Meldrum and H. Cölfen, *Chem. Rev.*, 2008, **108**, 4332–4432.
23 C. Claude, B. Garetz, Y. Okamoto and S. Tripathy, *Mater. Lett.*, 1992, **14**, 336–342.
24 J. Kim, J. L. Plawsky, R. LaPeruta and G. Korenowski, *Chem. Mater.*, 1992, **4**, 249–252.
25 J. F. Rabek, *Photochemistry and photophysics*, CRC Press, 1991.
26 J. George and K. G. Thomas, *J. Am. Chem. Soc.*, 2010, **132**, 2502–2503.
27 M. Hentschel, M. Schäferling, T. Weiss, N. Liu and H. Giessen, *Nano Lett.*, 2012, **12**, 2542–2547.
28 A. Ahniyaz, Y. Sakamoto and L. Bergström, *Proc. Natl. Acad. Sci. U. S. A.*, 2007, **104**, 17570–17574.
29 M. Giersig and M. Hilgendorff, *Eur. J. Inorg. Chem.*, 2005, 3571–3583.
30 W. Gao, X. Feng, A. Pei, C. R. Kane, R. Tam, C. Hennessy and J. Wang, *Nano Lett.*, 2013, **14**, 305–310.
31 H. Wang and M. Pumera, *Chem. Rev.*, 2015, **115**, 8704–8735.
32 C. Lizandara-Pueyo, S. Dilger, M. R. Wagner, M. Gerigk, A. Hoffmann and S. Polarz, *CrystEngComm*, 2014, **16**, 1525–1531.
33 J. Yin, Q. Lu, Z. Yu, J. Wang, H. Pang and F. Gao, *Cryst. Growth Des.*, 2009, **10**, 40–43.